IUST
Iran University of
Science and Technology

Iranian Journal of Electrical and Electronic Engineering

Journal Homepage: ijeee.iust.ac.ir

Research Paper

# Comparison of Radial Flux Air-cored Synchronous Superconducting Machine Topologies

S. Hasanzadeh*(C.A.), M. Yazdanian*, and S. M. Salehi*

**Abstract:** Over the past four decades of developing superconducting machines, many topologies have been suggested. The most successful topology of high-power superconducting (HPS) machines is an air-cored radial flux synchronous machine. There are two possible topologies for this type of machine, rotational field, and stationary field. In this paper, the relative advantages and disadvantages of these topologies are compared in detail. Analytical study of these topologies shows that the inversed machine topology leads to more efficient high-temperature superconductor (HTS) wire utilization and hence more economical production. In order to confirm the result obtained by analytical calculations, 2-D finite element model (FEM) of the machine is utilized.

**Keywords:** Finite Element Model (FEM), Inversed Topology, Machine Design, Superconducting Machine.

## 1 Introduction

A more significant flux density of field winding or higher linear current density of the armature leads to the higher power density machine. In conventional machines, the saturation of stator Iron-tooth limits the flux density [1-4]. Also, the linear current density of the armature is restricted by losses and mechanical considerations [5, 6]. Eliminating the iron core of the machine needs a large electromagnetic force which practically copper field winding cannot provide due to losses and volume restrictions. HTS wires can conduct about 100 times the electrical current of copper wire of the same dimensions with the ignorable loss [7]. The conduction enables manufacturing the air-cored superconducting machines using superconducting field winding and copper armature winding [8, 9]. Therefore, non-magnetic stator tooth and rotor leads to the smaller and lighter machine. Also, a higher efficiency level can be obtained by eliminating copper loss of field winding and iron-tooth loss [10].

Based on the arrangement of field and armature windings, the synchronous machine may be classified into rotating-field type (RFT) and rotating armature type (RAT) [11]. In the RFT, the field winding is placed on the rotor, which field current is supplied from the exciter via two slip-rings, and AC armature winding is placed on the stator [12]. In the alternate type (RAT), which is sometimes called “inversed topology”, the field winding is placed on the stator, whereas AC armature winding is placed on the rotor [13]. In this topology, the electrical input or output in the motor or generator is supplied to or taken from rotating armature respectively using three or four slip-rings. The main disadvantage of inversed machine topology is that transmission of large currents via brushes is not feasible for very large ratings. Therefore, it is limited to small and average rating machines.

In this paper, the air-cored radial flux synchronous machine is studied. This arrangement has some advantages for superconducting field winding machines. Because of these advantages, there is more interest in superconducting synchronous electric machines. Still, high manufacturing costs, especially HTS tape price, is the main cost of the motor is a big problem to commercialize them. Second-generation wires promised lower costs and better performance, but the HTS wires are expensive. Therefore, the application of superconducting machines is limited to exceptional

Iranian Journal of Electrical and Electronic Engineering, 2022.
Paper first received 17 September 2021, revised 25 February 2022, and accepted 13 March 2022.
* The authors are with the Electrical and Computer Engineering, Qom University of Technology, Iran.
E-mails: hasanzadeh@qut.ac.ir, m.yazdanian@gmail.com, and sm.salehi3@gmail.com.
Corresponding Author: S. Hasanzadeh.
https://doi.org/10.22068/IJEEE.18.3.2288

cases in which volume and weight are essential, such as offshore wind turbine generators and ship propulsion motors and generators. Optimum utilization of HTS wire significantly reduces manufacturing costs. This paper compares two possible topologies of stationary outside synchronous machine (field inside and field outside). The inside rotational field is a common structure, but analytical study and FEM results show that the stationary outside field would have been a better choice for superconducting machines.

## 2 Analysis of Air-cored Machine

The air-cored machine is made up of three major parts, including field winding, armature winding, and magnetic shield. The front view of the simplified machine model is illustrated in Fig. 1. It is assumed that the machine is infinitely long in the z-axis direction, and the field winding carries an ideal current distribution of $A\sin(p\theta)$. In this condition, the flux density can be calculated in the two-dimensional plane. In order to solve the flux density, the field winding is modeled by a current sheet at its mean winding radius ($r_0$). Therefore, the radial and tangential flux density inside the magnetic shield at the desired point in cylindrical coordination ($r$, $\theta$) can be expressed by relations (1) and (2), respectively.

$$r > r_0, \quad \begin{cases} B_r = \dfrac{\mu_0 A}{2}\sigma_{r-out}\left(\dfrac{r_0}{r}\right)^{p+1}\cos(p\theta) \\ B_\theta = \dfrac{\mu_0 A}{2}\sigma_{\theta-out}\left(\dfrac{r_0}{r}\right)^{p+1}\sin(p\theta) \end{cases} \tag{1}$$

$$r < r_0, \quad \begin{cases} B_r = \dfrac{\mu_0 A}{2}\sigma_{r-in}\left(\dfrac{r}{r_0}\right)^{p-1}\cos(p\theta) \\ B_\theta = -\dfrac{\mu_0 A}{2}\sigma_{\theta-in}\left(\dfrac{r}{r_0}\right)^{p-1}\sin(p\theta) \end{cases} \tag{2}$$

where $\mu_0$, $A$ and $p$ are permeability in free space, maximum current sheet density of sinusoidal field winding, and pole pair numbers, respectively. The influence of the magnetic shield is shown by $\sigma$, which can be calculated as follows.

$$\sigma_{r-in} = \sigma_{\theta-in} = 1 + \eta\lambda_S\left(\frac{r_0}{r_{S1}}\right)^{2p} \tag{3}$$

$$\sigma_{r-out} = 1 + \eta\lambda_S\left(\frac{r}{r_{S1}}\right)^{2p} \tag{4}$$

$$\sigma_{out} = 1 - \eta\lambda_S\left(\frac{r}{r_{S1}}\right)^{2p} \tag{5}$$

wherewith relative permeability of $\mu_s$, the inner radius of $r_{s1}$, and outer radius of $r_{s2}$.

$$\lambda_S = (\mu_s - 1)/(\mu_s + 1) \tag{6}$$

$$\eta = \left[1 - \left(\frac{r_{S1}}{r_{S2}}\right)^{2p}\right] / \left[1 - \lambda_S^2\left(\frac{r_{S1}}{r_{S2}}\right)^{2p}\right] \tag{7}$$

It may be noticed that we never have the sinusoidal distribution of field winding. In this case, a desired periodic winding can be represented by the Fourier series of current sheets as (8).

$$\sum_{n=1}^{\infty} A_n \sin(np\theta) \tag{8}$$

In this paper, without loss of generality for simplification, a pure sinusoidal distribution of current is considered. The machine appearance power can be written as:

$$S_i = \frac{4\pi^2}{\sqrt{2}} n_{syn} k_{ws1} A_a B_{rf} l r_a^2 \tag{9}$$

where $n_{sync}$, $A_a$, $B_{rf}$, $l$, and $r_a$ are synchronous speed, the linear current density of armature, the radial component of the field flux density at the mean radius of armature winding, machine effective length, and stator mean radius.

## 3 Comparison of Topologies

As mentioned earlier, there are two possible topologies for radial flux air-cored synchronous machines. This section compares these topologies in different aspects, including magnetic flux density, cooling system, mechanical design, iron loss, and rotor energizing. Therefore the following assumptions are made:

1) For both machines, the same length of the superconductor is used in the field winding.
2) For both machines, the same length of copper wire is used in the armature winding.
3) The inner radius of the magnetic shield ($r_{s1}$) is the same.
4) Field and armature windings can be paced in radiuses $r_1$ and $r_2$ or $r_2$ and $r_1$ where $r_1 < r_2$.

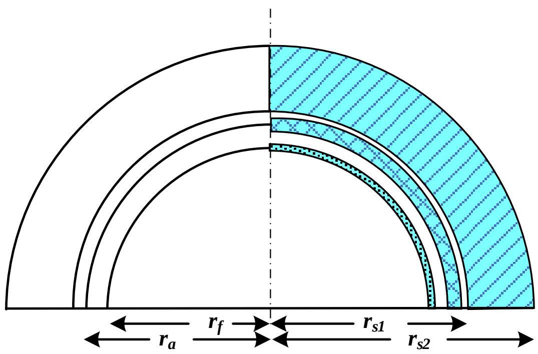


**Fig. 1** General machine model.

It can be shown that the maximum sheet current density of the same length of wire that carries a constant current is inversely proportional to the radius of the winding position. This can be shown as follows.

$$A_2 = \frac{r_1}{r_2} A_1 \tag{10}$$

## 4 Power Density

As shown above, the power of the machine is proportional to the flux density of field winding. Equations (1) and (2) can describe the flux density of field winding in the inner and outer regions of winding, respectively. Substituting $r_1$ and $r_2$ instead of $r_0$ and $r$ respectively in (1) gives flux density in armature radius in the case of RFT synchronous machine and similarly substituting $r_1$ and $r_2$ instead of $r$ and $r_0$ respectively in (2) gives the flux density in armature radius in the RAT synchronous machine. These expressions show that the radial flux density decreases more rapidly outside the winding than inside it. Using the same length of superconductor wire in RFT and RAT machines, the maximum radial flux density produced by the field winding at the mean of armature winding radius.

$$B_r = \frac{\mu_0 k}{2r_1}\left[1+\eta\lambda_S\left(\frac{r_2}{r_{S1}}\right)^{2p}\right]\left(\frac{r_1}{r_2}\right)^{p+1} \tag{11}$$

$$B_r = \frac{\mu_0 A}{2r_2}\left[1+\eta\lambda_S\left(\frac{r_2}{r_{S1}}\right)^{2p}\right]\left(\frac{r_1}{r_2}\right)^{p-1} \tag{12}$$

where

$$k = A_1 r_1 = A_2 r_2 \tag{13}$$

As can be seen, iron shield influence in both cases is the same, but in RAT machines, higher radial flux density can be achieved with $r_2/r_1$ ratio relative to RFT machines. Substituting radial flux and linear current density of RFT and RAT machines into (9) shows that these two arrangements have the same power density. In order to more detail study these two topologies, a typical two-pole pair air-cored machine is considered. In the first case, the field winding is located inside the armature winding, having $r_f / r_{s1}$ = 0.85 and $r_a / r_{s1}$ = 0.95. In the second case, the position of the armature and the field winding has been changed. Using (11) and (12) radial flux density versus normalized radius can be obtained. A 2-D finite element model of the machine is used in order to verify the analytical results. Both analytical and FEM calculated results are depicted in Fig. 2. The results show very good agreement except in the region near the field winding, which is outside the scope of this paper. In this figure, the flux density decreases linearly in the field's interior region, but in the outer region, field is decreasing more rapidly. The radial flux densities of field winding in the corresponding armature radius are shown by asterisk.

## 5 Magnetic Shield

The magnetic shield covers the entire machine and significantly decreases the magnetic field pollution around the machine. Also, the presence of a magnetic shield can boost the magnetic field maximum by the factor of two. Equations (3) to (7) describe the magnetic shield influence on radial and the tangential component of the magnetic shield. As can be seen in these equations, a magnetic shield is often made of laminated iron. Therefore, the thickness of the magnetic shield is proportional to the magnetic flux of field winding.

$$B_r\left(r_{S1}\right) = \frac{\mu_0 k}{2r_f}\left(1+\eta\lambda_S\right)\left(\frac{r_f}{r_{S1}}\right)^{p+1} = \frac{\mu_0 k}{r_{S1}^{p+1}} r_f^p \tag{14}$$

This equation indicates that the magnetic field of the magnetic shield will increase if the field is located near the shield. In other words, the rotary armature topology needs a thicker magnetic shield which results in higher weight. Also, Fig. 3 shows the maximum radial flux density produced by field winding (which occurs at the winding) made up with the same superconducting wire length for different pole pairs. As shown in Fig. 3,

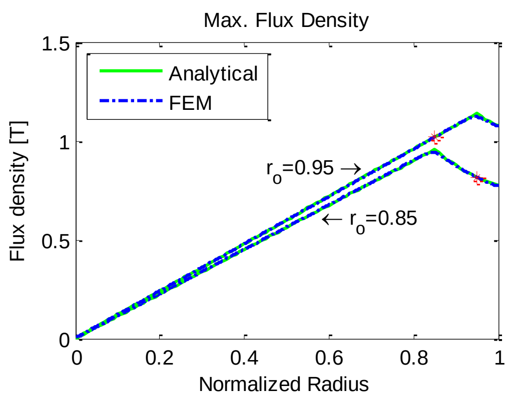


**Fig. 2** Flux density of field winding in two positions by analytical and FEM calculation.

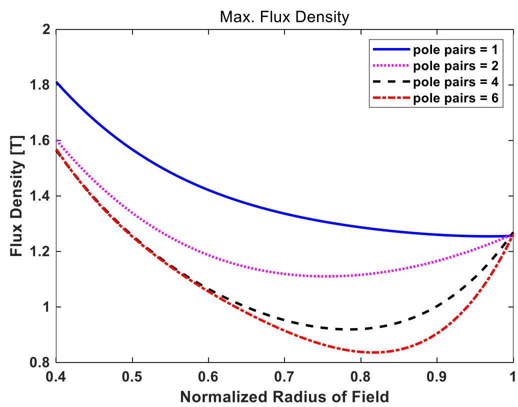


**Fig. 3** Maximum radial flux density.

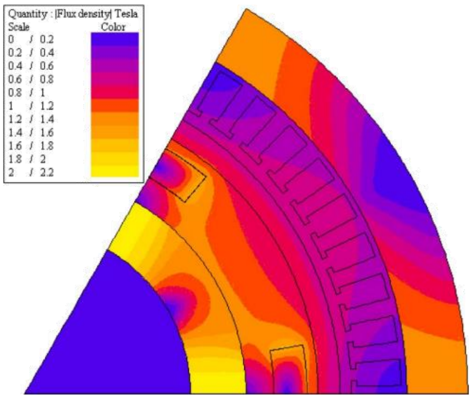


**Fig. 4** Magnetic flux density.

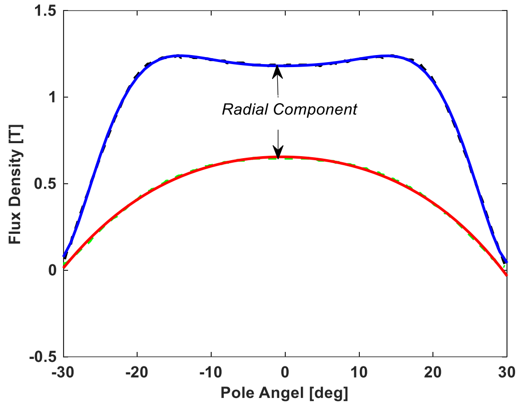


**Fig. 5** Finite-element results and analytical calculations in radial component of the machine.

increasing pole pairs result in lower flux density while the same length of superconductor wire is used. In addition, the magnetic flux density in different regions of the aforementioned typical machine is calculated. In addition, the machine is simulated with the FEM, which the magnetic flux density of the machine in a 2-D plate is depicted in Fig. 4. In order to compare the FEM and analytical results, the tangential and radial components of the magnetic flux density over a pole are considered. Therefore, the flux density in different radials are calculated, some of which are depicted in Fig. 5. In this figure, the solid lines represent the analytical results, and the dash-dot lines represent FEM results. As shown in this figure, the FEM and analytical results have good agreement in the air, but there is some mismatch problem in the iron.

## 6 Cooling

The resistance of superconductor wires will be disappeared below the temperature called critical temperature. This temperature depends on the current and external magnetic field and doesn't exceed a few tens of Kelvins. The main part of the cooling system is the compressor and cold-head. The cold-head cools down the cooling liquid or gas, circulates the superconductor wires, and absorbing winding heat. The circulation of cooling liquid or gas in inverse topology is simple, but a mechanical part called rotary joint is needed in conventional. The rotary joint connects the stationary parts of the cooling system to the rotor and makes possible cooling liquid or gas circulation. In this case, sealing of rotary joint is very important because the leakage can cause some problems. In low-speed superconductor machines such as direct drive ship propulsion motors, the design and manufacture of the rotary joint are simpler than high-speed machines. Often PTFE derivatives are used to seal rotary joints, which has many advantages such as low thermal conductivity and good stability in low temperatures. Also, PTFE has one of the lowest coefficients of friction against other solids.

## 7 Mechanical Design

The machine's torque is produced when a force $F$ is exerted on the rotor winding according to the Lorentz force. This torque-producing force is the cross-product of the current $I$ and the flux density. In the air-cored machines winding should tolerate mechanical stresses themselves. Therefore, analysis of mechanical stresses is inevitable. Often the superconductor wires are laminated with thin strips of metal to enhance mechanical properties. Non-magnetic metals are used to reinforce the superconducting wire, such as stainless steel, brass, or copper. The stress on the rotor winding has both tangential and radial components, while stator winding has only tangential components. The tangential torque of the rotor and stator are equal; therefore, the tangential component of force on the rotor is more than the stator. Also, rotor winding should be capable of withstanding a large number of centrifugal forces. The stress $\sigma_{mec}$ caused by the centrifugal force in the rotor is proportional to the square of the angular speed

$$\sigma_{mec} = C\rho r_r^2\Omega^2 \tag{15}$$

For a thin cylinder, $C$ is approximately equal to the unit, $\Omega$ is the mechanical angular speed (radians per second), $\rho$ is the material density (grams per cubic centimeter), $v$ is Poisson's ratio (i.e., the ratio of lateral contraction to longitudinal extension in the direction of the stretching force).

The thickness of superconducting wire depends on the lamination while it doesn't tailor superconducting property. This may cause significant force differences on armature and field windings. Therefore, the mechanical tangential force on the winding placed on the stator may be significantly low. It is necessary to note that a large amount of winding is required for large rating machines. Hence if the armature is rotating, large mechanical input is needed to drive prime mover, and there may be significant frictional losses mechanical losses.

## 8 Iron Loss

The synchronous machine is consisting of two main windings, the armature winding and field winding. A DC current should supply the field winding to provide a constant magnetic field as permanent magnets. The armature winding consists of three winding, when excited by a 3-phase supply, creates a rotating magnetic field relative to the windings frame. Often the magnetic core of the electric machine is built of laminated steel, which is optimized to produce small energy dissipation in an alternating magnetic field. However, the iron loss is a significant part of electric machine losses. In conventional topology, the armature is placed on the stator, which imposes a rotational magnetic field on the iron shield. The armature winding in the inversed topology rotates at the synchronous speed in the inverse direction of mechanical rotation. Therefore, a constant magnetic field is produced in the magnetic iron shield except for the transient condition. In other words, the inversed topology has no iron losses in steady-state operation. In loss calculation of brushes, the resistance of brushes is negligible because current density in brushes is very low, but the contact voltage drops of brushes, which strongly depends on the variety of parameters such as material and applied pressure (typically 0.2-1.5 V), causes significant losses. The brushes losses for conventional and inversed topologies can be obtained by (16)

$$P_b = 2\times\left(I_f \times V_{drop}\right)3\times\left(\frac{\sqrt{2}}{\pi} I_{ph} \times V_{drop}\right) \tag{16}$$

where $I_{ph}$ is the rms value of phase current. Therefore, the preferred topology can be selected, considering the current of field and armature winding.

## 9 Conclusion

In this paper, the air-cored radial flux Superconducting synchronous machine is studied. The relative advantages and disadvantages of the synchronous machine topologies are compared in detail. Analytical study of these topologies shows that the inversed machine topology leads to more efficient (HTS) wire utilization and hence more economical production. In order to confirm the result obtained by analytical calculations, 2-D (FEM) of the machine is utilized. Future work can focus on experimental results and comparisons between both types of machines from different aspects such as AC losses, cooling design, weight estimation, etc. In addition, 3-D (FEM) can be performed on machines and surveyed some issues such as the effects of end windings on torque production.

### Intellectual Property

The authors confirm that they have given due consideration to the protection of intellectual property associated with this work and that there are no impediments to publication, including the timing of publication, with respect to intellectual property.

### Funding

No funding was received for this work.

### CRediT Authorship Contribution Statement

**S. Hasanzadeh:** Conceptualization, Methodology, Software, Formal analysis, Writing - Original draft, Supervision. **M. Yazdanian:** Conceptualization, Methodology, Software, Formal analysis, Writing - Original draft. **S. M. Salehi**: Revise & editing, Investigation.

### Declaration of Competing Interest

The authors hereby confirm that the submitted manuscript is an original work and has not been published so far, is not under consideration for publication by any other journal and will not be submitted to any other journal until the decision will be made by this journal. All authors have approved the manuscript and agree with its submission to "Iranian Journal of Electrical and Electronic Engineering".

### References

[1] Y. Li, Z. Q. Zhu, and G. J. Li, "Influence of stator topologies on average torque and torque ripple of fractional-slot SPM machines with fully closed slots," *IEEE Transactions on Industry Applications*, Vol. 54, No. 3, pp. 2151–2164, 2018.

[2] D. Dezhin, N. Ivanov, K. Kovalev, I. Kobzeva, and V. Semenihin, "System approach of usability of HTS electrical machines in future electric aircraft," *IEEE Transactions on Applied Superconductivity*, Vol. 28, No. 4, pp. 1–5, 2017.

[3] S. Xue, A. S. Thomas, Z. Zhu, L. Huang, A. Duke, R. E. Clark, and Z. Azar, "Stator optimization of wind power generators with high-temperature superconducting armature windings and permanent magnet rotor," *IEEE Transactions on Applied Superconductivity*, Vol. 31, No. 2, pp. 1–10, 2020.

[4] S. Xue, A. S. Thomas, Z. Zhu, L. Huang, A. Duke, R. E. Clark, and Z. Azar, "Influence of coil location and current angle in permanent magnet wind power generators with high-temperature superconducting armature windings," *IEEE Transactions on Applied Superconductivity*, Vol. 31, No. 1, pp. 1–10, Jan. 2021.

[5] P. Lasek, K. Habelok, and M. Stepien, "Armature winding analysis for high-temperature superconducting PM-excited AC machines," *International Journal of Applied Electromagnetics and Mechanics*, Vol. 64, No. S1, pp. S269–S278, 2020.

[6] A. Lehikoinen, J. Ikäheimo, A. Arkkio, and A. Belahcen, "Domain decomposition approach for efficient time-domain finite-element computation of winding losses in electrical machines," *IEEE Transactions on Magnetics*, Vol. 53, No. 5, pp. 1–9, 2017.

[7] H. Zhang, Z. Wen, F. Grilli, K. Gyftakis, and M. Mueller, "Alternating current loss of superconductors applied to superconducting electrical machines," *Energies*, Vol. 14, No. 8, p. 2234, 2021.

[8] K. H. Shin, T. K. Bang, J. Y. Choi, H. W. Cho, and K. S. Haran, "Detailed analytical modeling for electromagnetic performance in actively shielded superconducting machines," *AIP Advances*, Vol. 11, No. 2, p. 025306, 2021.

[9] H. Zhang, Q. Li, O. Ubani, and M. Mueller, "High temperature superconducting halbach array topology for air-cored electrical machines," *Journal of Physics: Conference Series*, Vol. 1559, No. 1, p. 012140, 2020.

[10] M. Biasion, J. F. Fernandes, S. Vaschetto, A. Cavagnino, and A. Tenconi, "Superconductivity and its application in the field of electrical machines," in *IEEE International Electric Machines & Drives Conference (IEMDC)*, pp. 1–7, 2021.

[11] C. H. Zhao and Y. G. Yan, "A review of development of hybrid excitation synchronous machine," in *Proceedings of the IEEE International Symposium on Industrial Electronics*, Vol. 2, pp. 857–862, 2005.

[12] V. Ostović, *The art and science of rotating field machines design: A practical approach*. Springer, 2016.

[13] S. H. Park, Y. Kim, S. Lee, W. Kim, J. Y. Lee, J. Lee, and K. Choi, "Characteristics of rotating armature type high temperature superconducting generators with dual field windings for the wind turbine," *IEEE Transactions on Applied Superconductivity*, Vol. 25, No. 3, pp. 1–5, 2015.

**S. Hasanzazdeh** was born in Shirvan, Iran, in 1981. He received the B.Sc. degree in Electrical Engineering from Shahroud University of Technology, Shahroud, Iran, in 2003, and the M.Sc. and Ph.D. degrees in Electrical Engineering from University of Tehran (UT), Tehran, Iran, in 2006 and 2012, respectively. His M.Sc. thesis and Ph.D. dissertation have been conducted in the field of High Voltage Engineering and Wireless Power Transfer (WPT), respectively. In 2013, he joined the Department of Electrical and Computer Engineering, Qom University of Technology, as an Assistant Professor. Dr. Hasanzadeh is an Editorial Board of the Power Electronics Society of Iran (PELSI). He is a TPC member of the IEEE Power Electronics & Drives: Systems and Technologies Conference (PEDSTC). He was the recipient of the top research prize of the Qom University of Technology in 2019. Also, He was recognized as an Outstanding Lecturer at the Qom University of Technology in 2020. He is currently the Dean of the Department of Electrical and Computer Engineering (ECE), Qom University of Technology. His current research interests include power electronics, electrical machines, wireless power transfer, and high voltage engineering.

**M. Yazdanian** was born in Isfahan, Iran, in 1981. He received the B.Sc. degree from the University of Yazd, Yazd, Iran, in 2004, the M.Sc. degree from the University of Tehran, Tehran, Iran, in 2007, and the Ph.D. degree from the Sharif University of Technology, Tehran, Iran, in 2014, all in Electrical Engineering. During his graduate studies, he completed an internship with ABB Corporation Research Center, Baden, Switzerland, working on vacuum circuit breakers. His research interests include superconductivity and its application in power, design, and modeling of power electronic circuits, machine design, renewable energy, and high-voltage engineering.

**S. M. Salehi** received the B.Sc. degree from Shahab Danesh University, Qom, Iran, and the M.Sc. degree from Qom University of Technology, Qom, in 2012 and 2016, respectively, both in Electrical Engineering. His research interests include design, modeling, and control of power electronics converters and their applications in electrical traction systems.